Electrodeposition of Ni–Co double hydroxide composite nanosheets on Fe substrate for high-performance supercapacitor electrode

Liyang Jiang, Yanwei Sui, Jiqiu Qi ✉, Yuan Chang, Yezeng He, Fuxiang Wei, Qingkun Meng, Zhi Sun

School of Materials Science and Engineering, China University of Mining and Technology, Xuzhou 221116, People's Republic of China
✉ *E-mail: flower_cumt@outlook.com*

Published in Micro & Nano Letters; Received on 22nd July 2016; Revised on 31st August 2016; Accepted on 2nd September 2016

In this work, Ni–Co double hydroxide composite nanosheets with network structure grown on conductive substrate of Fe foil was synthesised by a facile electrochemical deposition method. This structure is responsible for high electrochemical performance with specific capacitance of 853.7 F g^{-1} at the current density of 1.0 A g^{-1} and long-term cycling stability of 85% capacitance retention at 4 A g^{-1} after 1000 cycles. These results suggest that low-cost Fe foil can be used as effective collector for high performance supercapacitors.

1. Introduction: In recent years, with the increasing demand in electric energy storage for vehicles and mobile electronics, supercapacitors have attracted extensive research interests due to their high power density, fast charging–discharging capability, low maintenance costs, and long cycle life [1, 2]. To date, various materials, including carbon material, metal oxide/hydroxide and conducting polymers have been widely used as supercapacitor electrodes [3–6]. Pseudocapacitors based on reversible faradaic redox reaction have been demonstrated to be more excellent in specific capacitance [7, 8]. In this kind of supercapacitor, electrode materials mainly consist of transit metal oxides and/or hydroxides, especially nickel oxides and/or hydroxides and cobalt oxides and/or hydroxides [9, 10]. As we know, Ni foam is the most common current collector [11]. Recently, Ti foils have been developed and used as current collector in [12, 13]. If Fe foils can be applied in supercapacitor electrodes, the fabrication cost of these electrodes should decrease. However, to the best of our knowledge, there is still no research report about $Co(OH)_2$ and/or $Ni(OH)_2$ on cheap iron foils.

Herein, Ni–Co double hydroxide composite grown on Fe foil was designed and synthesised using electrochemical deposition in this Letter. The aim is to investigate the structure and electrical properties of the composite.

2. Experimental procedure: All medicines for the analysis in this Letter were of analytical grade and used without further purification. Ni–Co double hydroxide composite grown on Fe foil was prepared via electrochemical deposition. This experiment was performed with a CHI660e electrochemical station (Chenhua, Shanghai) that was connected with a three-electrode cell. Fe foil with size of 1×1.5 cm^2 and thickness of 0.1 mm, Pt plate with size of 1×2 cm^2 and mercuric oxide electrode were used working electrode, counter electrode and reference electrode, respectively. Before the experiment, the iron foils were polished by sand paper and then washed with acetone, distilled water and alcohol in an ultrasonic wave cleaner for 15 min, respectively. 0.58 g $Co(NO_3)_2{\cdot}6H_2O$, 0.29 g $Ni(NO_3)_2{\cdot}6H_2O$ and 1.07 g NH_4Cl were dissolved in 100 ml deionised water to form a transparent pink solution. Finally, Ni–Co double hydroxide composite was cathodically electrodeposited on the Fe substrate in the solution with a constant potential of −0.7 V for 1 h. After washing, a layer of green-coloured product can be seen on the surface of Fe foil.

The X-ray diffraction (XRD, D8 Advance, Bruker, Germany) was used to characterise the structure of products. The morphology of the product was observed by field emission scanning electron microscope (SEM, Hitachi SU-8000) and transmission electron microscope (TEM, FEI Tecnai G2 F20). The electrochemical performance of the as-prepared sample was evaluated by cyclic voltammetry (CV) and galvanostatic charge–discharge tests with an electrochemical workstation (CHI660E, Chenhua) that was connected with a three-electrode system, which is same to that used in electrochemical deposition system.

3. Results and discussion: The XRD pattern of Ni–Co double hydroxide composite grown on Fe substrate is shown in Fig. 1. Two clear peaks of Fe foil can be observed at 44.7° and 65° from Fig. 1, corresponding to the crystallographic planes of (110) and (200), respectively. The peaks of $Co(OH)_2$ are in good agreement with standard powder diffraction patterns of α-$Co(OH)_2$ and similar results have been reported in [14, 15].

It should be noted that the peaks of (003), (006), (101) and (110), corresponding to α-$Ni(OH)_2$, are totally overlapped with those of α-$Co(OH)_2$ (Fig. 1) [16, 17]. The plane spacing of (003) peak was calculated to be 0.787 nm, very close to the that of sole α-$Co(OH)_2$ (0.792 nm) or α-$Ni(OH)_2$ (0.779 nm). These confirm that Ni–Co double hydroxide composite grown on Fe foil was successfully fabricated through electrochemical deposition. No other diffraction peaks are detected from Fig. 1, meaning the high purity of the as-prepared Ni–Co double hydroxide composite.

Fig. 2 displays the morphology of the as-prepared Ni–Co double hydroxide composite. In Fig. 2*a*, Ni–Co double hydroxide composite grew in nanosheet structure with flower shape.

The presence of these pores should be beneficial for the expanding of the contact area between electrolyte and active materials. In addition, this kind of network structure promotes the electron transportation in the internal of Ni–Co double hydroxide composite. The thicknesses of the nanosheets varied from 30 to 40 nm.

The morphology of Ni–Co double hydroxide composite was further investigated by TEM, as illustrated in Fig. 3. It can be seen from Fig. 3*a* that the composite exhibits sheet-like shape, which is consistent with the observation from SEM images in Fig. 2.

In addition, many infinitesimal nanoparticles were attached on the surface of Ni–Co double hydroxide composite (Fig. 3*a*). It seems that the obtained Ni–Co double hydroxide composite nanosheets were composed of many nanoparticles. Fig. 3*b* shows that the diffraction spots of Ni–Co double hydroxide composite in Fig. 3*a* are arranged on many circles, confirming the polycrystalline structure of the nanosheets. The pattern in Fig. 3*b* can be nearly

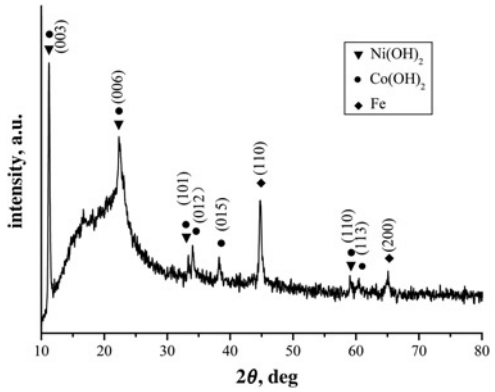

Fig. 1 *XRD pattern of Ni–Co double hydroxide composite grown on Fe foil*

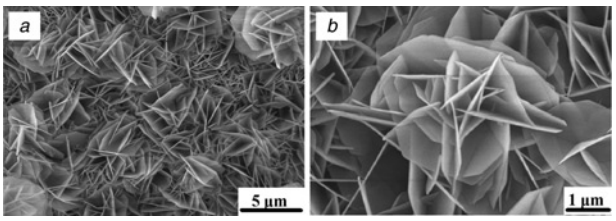

Fig. 2 *a, b SEM images showing the morphology of Ni–Co double hydroxide composite*

indexed as (003) and (006) diffractions of α-$Co(OH)_2$ and α-$Ni(OH)_2$.

To evaluate the electrochemical performance of the Ni-Co double hydroxide composite grown on Fe substrate, a series of electrochemical tests were conducted. Fig. 4*a* shows the CV curves of

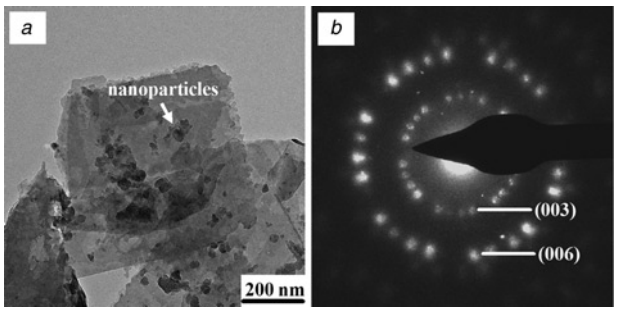

Fig. 3 *Morphology of Ni–Co double hydroxide composite was further investigated by TEM*
a TEM image of the as-prepared Ni–Co double hydroxide composite
b Selected area pattern of Ni–Co double hydroxide in Fig. 3*a*

Ni–Co double hydroxide composite electrode and Fe foil electrode in a 1.0 M KOH solution at a scanning rate of 20 mV s^{-1}. Compared with the Ni–Co double hydroxide composite electrode, the signal of Fe foil is quite small, indicating that Fe foil was stable and contributes little to the total capacitance of the electrode. Fig. 4*b* displays the CV curves of the Ni–Co double hydroxide composite electrode at different scanning rates from 5 to 60 mV s^{-1} in the potential window of −0.2 to 0.6 V (versus Hg/HgO). All the CV curves show a pair of clear redox peaks, which reflects the Faradic reactions between M–O/M–O–OH (M represents Co or Ni) and OH^- [18, 19]. The detailed reactions between the electrode materials and the alkaline electrolyte are as follows

$$Ni(OH)_2 + OH^- \leftrightarrow NiOOH + H_2O + e^- \quad (1)$$

$$Co(OH)_2 + OH^- \leftrightarrow CoOOH + H_2O + e^- \quad (2)$$

$$CoOOH + OH^- \leftrightarrow CoO_2 + H_2O + e^- \quad (3)$$

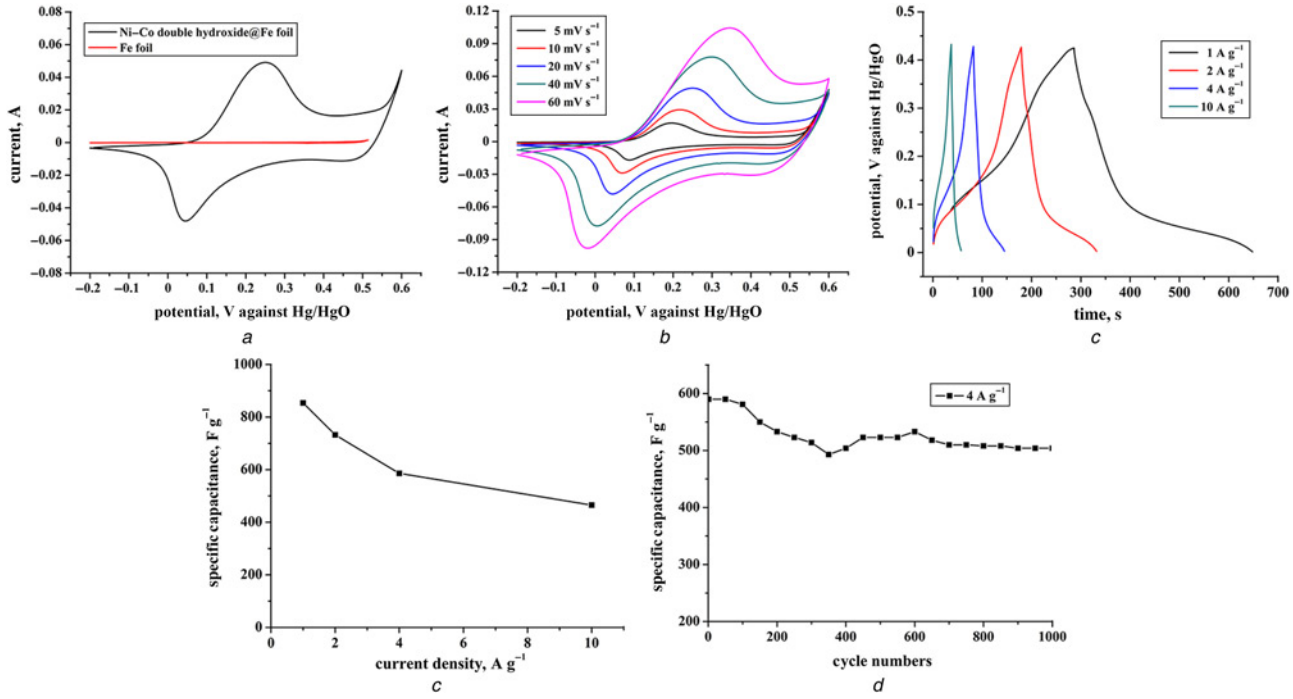

Fig. 4 *CV curves of*
a Ni–Co double hydroxide composites electrode and Fe foil electrode at a scanning rate of 20 mV s^{-1}
b Ni–Co double hydroxide composite electrode at various scanning rates of 5, 10, 20, 40 and 60 mV s^{-1}
c Galvanostatic charge–discharge curves of the composite electrode
d Specific capacitance of composite electrode
e Electrochemical cyclic stability of the composite

doi: 10.1049/mnl.2016.0485

The shape of CV curves is different from the regular rectangular characteristic of double-layer capacitors, meaning the pseudocapacitive feature of Ni–Co double hydroxide composite. With the increase of current density, it has a good electrochemical response (Fig. 4*b*).

The selected galvanostatic charge/discharge curves of the Ni–Co double hydroxide composite electrode at different current densities in the potential window of 0–0.4 V is shown in Fig. 4*c*. It is observed that the discharge voltage plateaus at around 0.1–0 V, which is consistent to the CV curves (Fig. 4*b*). The specific capacitances of the composite obtained from galvanostatic charge–discharge curves in Fig. 4*c* are 853.7, 732.4, 590.5 and 465.2 F g^{-1} at current density of 1, 2, 4 and 10 A g^{-1}, respectively, as shown in Fig. 4*d*. They were calculated according to the following equation

$$C_S = \frac{I \times \Delta t}{\Delta V \times m} \quad (4)$$

where C_S (F g^{-1}) is the specific capacitance, I (A) is the discharge current, Δt (s) is the discharge time, ΔV (V) is the potential window and the m (g) is the mass of the active materials. To the best of our knowledge, this specific capacitance is higher than some cobalt and nickel layered double hydroxide nanosheets on Ni foam materials (774 F g^{-1} at the current density of 0.2 A g^{-1}) reported by Wang *et al.* [20]. The cycling stability of the composite electrode is another important electrochemical property for supercapacitor. The cycling performance of the composite was measured at a high current density of 4 A g^{-1} for 1000 cycles. As shown in Fig. 4*e*, after 1000 cycles, the capacitance maintains 85% of the initial capacitance. It is worth mentioning that the capacitance decreases obviously after 350 cycles. Subsequently, the decreasing rate of the capacitance becomes very slow, which indicates that the transformation of α-Co$(OH)_2$ to β-Co$(OH)_2$ could happen in strong alkaline media during the cycle since α-Co$(OH)_2$ is metastable. The obvious degradation in capacitance in the first 350 cycles should be attributed to the transformation of α-Co$(OH)_2$ to β-Co$(OH)_2$. To enhance the cycling stability, the content of Co$(OH)_2$ should be controlled. Overall, the above results demonstrate that the Ni–Co double hydroxide composite grown on Fe foil has a high specific capacitance due to its network structure and large surface area, which is beneficial for the electrolyte transport and charge-transfer reactions.

4. Conclusion: Ni–Co double hydroxide composite grown on Fe foil was successfully fabricated using electrochemical deposition and used as an electrode for supercapacitor. The Ni–Co double hydroxide composite consisted of vertical stacking nanosheets with network structure, which favours electrolyte transport and provides more electroactive sites for fast energy storage. Due to this, the Ni–Co double hydroxide composite exhibited high electrochemical performance with specific capacitances of 853.7 F g^{-1} at current density of 1 A g^{-1} and long cycling stability of 85% of the initial capacitance after 1000 cycles at the current density of 4 A g^{-1}. It is believed that the as-synthesised Ni–Co double hydroxide composite deposited on Fe foil is a very promising candidate for high-performance supercapacitors.

5. Acknowledgments: This work was financially supported by the National Natural Science Foundation of China (grant nos. 51601220 and 51671214).

6 References

[1] Simon P., Gogotsi Y., Dunn B.: 'Where do batteries end and supercapacitors begin?', *Science*, 2014, **343**, pp. 1210–1211

[2] Li R., Wang S., Huang Z., *ET AL.*: '$NiCo_2S_4$@$Co(OH)_2$ core-shell nanotube arrays in situ grown on Ni foam for high performances asymmetric supercapcitors', *J. Power Sources*, 2016, **312**, pp. 156–164

[3] Zhao Y.F., Ran W., He J., *ET AL.*: 'High-performance asymmetric supercapacitors based on multilayer MnO_2/graphene oxide nanoflakes and hierarchical porous carbon with enhanced cycling stability', *Small*, 2015, **11**, pp. 1310–1319

[4] Zhang Y.L., Si L., Zhou B., *ET AL.*: 'Synthesis of novel graphene oxide/pristine graphene/polyaniline ternary composites and application to supercapacitor', *Chem. Eng. J.*, 2016, **288**, pp. 689–700

[5] Chang Y., Sui Y.W., Qi J.Q., *ET AL.*: 'Hierarchical Ni_3S_2 nanosheets coated on mesoporous $NiCo_2O_4$ nanoneedle arrays as high-performance electrode for supercapacitor', *Mater. Lett.*, 2016, **176**, pp. 274–277

[6] Shuvo M.A.I., Tseng T.L., Md. Ashiqu R.K., *ET AL.*: 'Nanowire modified carbon fibers for enhanced electrical energy storage', *J. Appl. Phys.*, 2013, **114**, p. 104306

[7] Zhou J., Huang Y., Cao X.H., *ET AL.*: 'Two-dimensional $NiCo_2O_4$ nanosheet-coated three-dimensional graphene networks for high-rate, long-cycle-life supercapacitors', *Nanoscale*, 2015, **7**, pp. 7035–7039

[8] Qi J.Q., Lu J., Sui Y.W., *ET AL.*: 'TiO_2/Fe_2O_3 composite obtained through oxidation of Ti-15Fe alloy foil for high-performance supercapacitor electrode', *Mater. Lett.*, 2016, **184**, pp. 34–37

[9] Yang Y., Li L., Ruan G.D., *ET AL.*: 'Hydrothermally formed three-dimensional nanoporous $Ni(OH)_2$ thin-film supercapacitors', *Acs Nano*, 2014, **8**, pp. 9622–9628

[10] Wang C.L., Qu H.L., Peng T., *ET AL.*: 'Large scale alpha-$Co(OH)_2$ needle arrays grown on carbon nanotube foams as free standing electrodes for supercapacitors', *Electrochim. Acta*, 2016, **191**, pp. 133–141

[11] Wei J.T., Lin G.N., Wang Y., *ET AL.*: 'Integrated carbon spheres on nickel foam as electrode for supercapacitors', *Micro Nano Lett.*, 2013, **8**, pp. 151–154

[12] Zheng Z., Chen J.J., Yoshida R., *ET AL.*: 'One-step synthesis of TiO_2 nanorod arrays on Ti foil for supercapacitor application', *Nanotechnology*, 2014, **25**, p. 435406

[13] Zhang G.Q., Wu H.B., Hoster H.E., *ET AL.*: 'Single-crystalline $NiCo_2O_4$ nanoneedle arrays grown on conductive substrates as binder-free electrodes for high-performance supercapacitors', *Energy Environ. Sci.*, 2012, **5**, pp. 9453–9456

[14] Liu Z., Ma R., Osada H., Osada M., *ET AL.*: 'Selective and controlled synthesis of α-and β-cobalt hydroxides in highly developed hexagonal platelets', *J. Am. Chem. Soc.*, 2005, **127**, (40), pp. 13869–13874

[15] Tang J., Liu D.Q., Zheng Y.X., *ET AL.*: 'Effect of Zn-substitution on cycling performance of alpha-$Co(OH)_2$ nanosheet electrode for supercapacitors's, *J. Mater. Chem. A*, 2014, **2**, pp. 2585–2591

[16] Lee J.W., Ahn T., Soundararajan D., *ET AL.*: 'Non-aqueous approach to the preparation of reduced graphene oxide/α-$Ni(OH)_2$ hybrid composites and their high capacitance behavior', *Chem. Commun.*, 2011, **47**, pp. 6305–6307

[17] Mavis B., Akinc M.: 'Cyanate intercalation in nickel hydroxide', *Chem. Mater.*, 2006, **22**, pp. 5317–5325

[18] Yang S.N., Cheng K., Ye K., *ET AL.*: 'A novel asymmetric supercapacitor with buds-like $Co(OH)_2$ used as cathode materials and activated carbon as anode materials', *J. Electroanal. Chem.*, 2015, **741**, pp. 93–99

[19] Li H.B., Yu M.H., Wang F.X., *ET AL.*: 'Amorphous nickel hydroxide nanospheres with ultrahigh capacitance and energy density as electrochemical pseudocapacitor materials', *Nat. Commun.*, 2013, **4**, p. 1894

[20] Wang C.H., Zhang X., Sun X.Z., *ET AL.*: 'Facile fabrication of ethylene glycol intercalated cobalt-nickel layered double hydroxide nanosheets supported on nickel foam as flexible binder-free electrodes for advanced electrochemical energy storage', *Electrochim. Acta*, 2016, **191**, pp. 329–336